

THE DER P 5 CRYSTAL STRUCTURE PROVIDES INSIGHT INTO THE GROUP 5 DUST MITE ALLERGENS

Geoffrey A. Mueller¹, Rajendrakumar A. Gosavi¹, Joseph M. Krahn¹, Lori L. Edwards², Matthew J. Cuneo¹, Jill Glesner³, Anna Pomés³, Martin D. Chapman³, Robert E. London¹, Lars C. Pedersen¹

From Laboratory of Structural Biology¹ and Protein Expression Core Facility² National Institute of Environmental Health Sciences, and INDOOR Biotechnologies Inc³, Charlottesville, VA.

Running head: Crystal Structure of Der p 5

Address correspondence to Geoffrey Mueller, Ph.D. 111 T.W. Alexander Drive, Research Triangle Park, NC, 27709. 919-541-3872 F: 919-541-5707; Email: mueller3@niehs.nih.gov

Group 5 allergens from house dust mites elicit strong IgE antibody binding in mite allergic patients. The structure of Der p 5 was determined by X-ray crystallography to better understand the IgE epitopes, to investigate the biologic function in mites, and for comparison with the conflicting published Blo t 5 structures, designated 2JMH and 2JRK in the protein data bank. Der p 5 is a three-helical bundle similar to Blo t 5, but the interactions of the helices are more similar to 2JMH than 2JRK. The crystallographic asymmetric unit contains three dimers of Der p 5 that are not exactly alike. Solution scattering techniques were used to assess the multimeric state of Der p 5 *in vitro*, and showed that the predominant state was monomeric, similar to Blo t 5, but larger multimeric species are also present. In the crystal, the formation of the Der p 5 dimer creates a large hydrophobic cavity of approximately 3000 Å³ that could be a ligand binding site. Many allergens are known to bind hydrophobic ligands, which are thought to stimulate the innate immune system and have adjuvant-like effects on IgE mediated inflammatory responses.

Introduction

Allergic diseases are estimated to afflict 20% of the world's population. House dust mites are a significant source of indoor allergens, which are associated strongly with extrinsic asthma (1). More than 20 allergen groups have been characterized from dust mites with varying levels of patient response (2). An important group is the group 5 allergens from dust mites, which elicit strong IgE binding in about 30% of mite allergic patients (3).

Two dust mite species *Dermatophagoides farinae* and *D. pteronyssinus* are found worldwide and predominate in climates with less humidity (*D. farinae*) or with seasonal fluctuations in humidity (*D. pteronyssinus*) (4,5). In tropical climates *Blomia tropicalis* is found in addition to *Dermatophagoides spp.* Indeed, asthmatic patients from Florida, Puerto Rico, and Brazil were found to be sensitized to both *D. pteronyssinus* and *B. tropicalis* (6). Patients from the United Kingdom who were sensitized only to *D. pteronyssinus* gave positive skin tests to *B. tropicalis* extract, but this apparent cross-reactivity was not due to the group 5 allergens (7). The group 5 allergens Der p 5 and Blo t 5 share 42% sequence identity and have been studied extensively for their cross reactivity in patients. Nearly all studies with recombinant allergens have concluded that the IgE antibody responses to the Group 5 allergens are species specific (6-9). Further, recent studies using polyclonal rabbit IgG antibodies raised against Der p 5 detected no binding with group 5 allergens from storage mites (i.e. *G. domesticus* or *L. destructor*) or *B. tropicalis* (10).

Structural characterization of allergens can provide important insights into the biologic function of allergens, which may influence their ability to cause IgE responses. Among dust mite allergens, many are proteases and this enzymatic property may be related to the chronic inflammation of the lung in asthmatic patients (11-13). Other studies suggested that the proteolytic activity enhanced IgE synthesis and/or skewed the immune response away from tolerance and towards an allergic response (14,15). However, it was reported that Der p 5 activated human airway-derived epithelial cells via a protease independent mechanism (16). Recently, crystallographic studies revealed that Der p 7 was distantly related to hydrophobic ligand binding proteins of the human innate immune system (17); this

relationship was not previously identified from sequence information alone. It was suggested that Der p 7 may co-opt the innate immune response into promoting allergenicity through the binding and delivery of hydrophobic ligands (17), as has been demonstrated for the mite allergen Der p 2 (18).

Previous structural studies of the Blo t 5 and related Der p 21 allergens have not identified a natural function in mites (19-21). Despite a preliminary X-ray report of Der p 5 crystals in 1998 (22), a definitive structure of Der p 5 has not been obtained. The structure of Blo t 5 was determined in two studies using NMR (19,20). Both studies confirmed the results of CD spectroscopy and bioinformatics predictions of other group 5 and the highly similar group 21 mite allergens, which suggested that the proteins were largely helical in nature (10,21-23). A superficial comparison of the two protein structures of Blo t 5 (2JMH and 2JRK in the protein data bank) shows two elongated proteins, both with three α -helices all in a parallel orientation, and a disordered N-terminus. A more careful comparison indicates that the folding topology of the two structures is different. Because of the degree of sequence identity between Der p 5 and Blo t 5, it was anticipated that the Der p 5 structure might shed light on the unexpected inconsistency between the two previously determined structures of Blo t 5. In the present study, we have solved the first crystal structure of Der p 5 at 2.8 Å resolution. The Der p 5 structure was found to adopt a space group in which the asymmetric unit contains six Der p 5 molecules in an apparent trimer of dimers. The structure presented here resolves the ambiguity between the two existing Blo t 5 structures and provides insights into the function of the group 5 and group 21 mite allergens.

Experimental Procedures

Expression and Purification- The construct designed for Der p 5 sought to reduce the number of disordered residues for crystallization based on previous NMR studies that indicated significant flexibility of the N terminal residues (19,20). A construct of Der p 5 encoding residues L34-V132 was inserted into a pGEX4T3 vector that had been modified to include a TEV restriction site between the BamHI and EcoRI site. Der p 5 was inserted

using the EcoRI and XhoI sites in the multi-cloning site. This vector was transformed into BL21(DE3)RIL cells. For protein expression of the GST-Der p 5 construct, 20mls of an overnight culture grown in LB + 100 μ g/ml Ampicillin at 37 C and 275 rpm, was added to each of six 1.8L Fernbach flasks containing 1L of LB media and 100 μ g/ml Ampicillin. These were placed on shakers at 37 C and 275 rpm until an OD600 of 0.8 was reached. The temperature was set to 18 C. When the temperature reached 22 C, IPTG was added to a final concentration of 500 μ M and cells were allowed to shake overnight at 18 C. Cells were pelleted at 4000 g. The cell pellets from 6 L of culture were resuspended in sonication buffer consisting of 25 mM Tris pH 7.5 and 500 mM NaCl to a final volume of 120 ml. Cells were sonicated on an ice/water bath for 3 bursts at 20 seconds each and then spun down for 35 min at 48,000 g. The supernatant was mixed with 12 ml of Glutathione Sepharose 4B resin and gently rocked at 4 C for 1 hour. The resin was pelleted at 500 g for 5 min and washed extensively with sonication buffer. Resin was transferred to the elution buffer consisting of 25 mM Tris pH 7.5 and 75 mM NaCl in a 50ml falcon tube. Der p 5 was eluted from the resin by adding 400 μ l of 1.5 mg/ml TEV protease to the falcon tube and gently rocked at 4 C overnight. The eluted protein was concentrated down to 40 mg/ml and loaded onto a 16/60 superdex200 column which was equilibrated in the elution buffer. Fractions containing purified Der p 5 were pooled and concentrated to 30.7 mg/ml and used for crystallization trials. For seleno-methionine labeled protein, the GST-Derp5 fusion protein was expressed in B834 (DE3) cells using minimal media supplemented with amino acids where seleno-methionine was substituted for methionine. Expression and purification procedures were similar to above except 2mM DTT was present in all buffers.

IgE binding- IgE antibody binding to the shorter Der p 5 construct was assessed by chimeric ELISA. Microtiter plates were coated at 4°C overnight with 10 μ g/ml of the short recombinant Der p 5 construct. Plates were blocked for 30 minutes with 1% BSA-PBS-0.05% Tween 20, pH 7.4 (BSA-PBS-T). A two hour incubation with sera (dilutions 1:2 and 1:10) was performed. All

other incubations were for one hour and plates were washed three times between steps with PBS-T. Bound IgE was detected using biotin labeled goat anti-human IgE (KPL, Gaithersburg, MD) at a 1:4,000 dilution. Streptavidin peroxidase was added at 250 $\mu\text{g/ml}$, followed by development with 1mM ABTS and 0.03% hydrogen peroxide as substrate. Plates were quantitated by measuring the OD at 405 nm and an O.D. >0.2 was considered positive. The sera from allergic patients were obtained from PlasmaLab International (Everett, WA), which operates in full compliance of Food and Drug Administration regulations. An informed donor's consent was obtained from each individual prior to the first donation.

Crystallization, data collection and refinement-

Crystals of native Der p 5 L34-V132 were obtained using the sitting and hanging drop vapor diffusion technique at room temperature by mixing 1 μl of protein with 1 μl of the reservoir solution consisting of 31.5% MPD (methylpentanediol) and 90mM Na/K phosphate buffer at pH 6.2. For data collection a crystal was taken directly from the sitting drop tray and frozen in liquid nitrogen. Data were collected at -180 C on an in-house Saturn92 CCD detector mounted on a 007HFmicromax generator equipped with VarimaxHF mirrors. Data were indexed and integrated and scaled in HKL2000 (24) and also scaled in XDS (25). Seleno-methionine labeled protein crystals were grown from similar conditions. Data were collected at wavelengths 0.97243 (peak) and 0.97943 (edge) at the SER-CAT beamline ID-22 at Argonne National Laboratory. All data were processed and scaled using HKL2000. Initial phases were obtained with a FOM of 0.29 by using the Auto_Sol routines in Phenix (26) which found 23 of the possible 36 seleno-methionine sites. The Auto_build routine in Phenix built 231aa (polyalanines) of the 608 present in the asymmetric unit producing a map with an FOM of 0.63. Manual model building and real space refinement in Coot (27) followed by refinement in CNS (28) and Phenix produced a model with six monomers in the asymmetric unit and an R_{work} of 25.8% and an R_{free} of 35.7%. The model was refined against the native data sets scaled in either HKL2000 or XDS using CNS and Phenix along with manual building in Coot. It was

determined that there was no benefit to the XDS refined data so the final reported structure was refined against HKL2000 processed data in Phenix using non-crystallographic symmetry restraints along with TLS refinement to obtain a model that includes all residues of the six Der p 5 molecules in the asymmetric unit with an R_{work} of 23.1% and an R_{free} of 28.7%. The structure was deposited in the protein data bank, PDB code 3MQ1.

SAXS Data Acquisition and Analysis- SAXS data were collected at room temperature on the X9 beam line at the National Synchrotron Light Source (Brookhaven National Laboratory) using the small Der p 5 construct. The wavelength of the beam was 0.855 \AA and the sample to detector distance was two meters. Der p 5 sample concentrations were 10, 5, and 2.5 mg/ml. Scattering data were circularly averaged and scaled to obtain a relative scattering intensity (I) as a function of momentum transfer vector, q ($q=[4\pi\sin\theta]/\lambda$), after subtraction of buffer scattering contributions. SAXS data on a standard protein, hen egg white lysozyme (14.2 kDa; Acros Organics, Morris Plains, NJ), were collected over a concentration series in the same capillary, and used for I_0 analyses.

All scattering data were analyzed using the Primus software package (29); the GNOM45 software package (30) was used for all $P(r)$ and I_0 analyses. The radius of gyration, R_g , and forward scattering, I_0 , were calculated from the second moment and the start of $P(r)$, respectively, where R_g is the root mean square of all elemental volumes from the center-of-mass of the particle, weighted by their scattering densities, and I_0 is directly proportional to the molar particle concentration multiplied by the square of the scattering particle molecular weight for particles with the same mean scattering density. Guinier plots for 10.0, 5.0, and 2.5 mg/ml Der p 5 samples were linear over a q -range of 0.010-0.0385 \AA^{-1} , 0.0095-0.044 \AA^{-1} , and 0.010-0.0495 \AA^{-1} respectively.

Initial results on Der p 5 indicated a particle size larger than a monomer, hence the data was analyzed for the presence of multiple species with the program OLIGOMER (31). Molecular models of possible solution conformers were generated from the crystallographic results, the

Blo t 5 structure 2JMH, and the SAXS model of Der p 21 (21).

RESULTS

IgE Binding to Der p 5- A total of 67 sera from allergic patients were tested for binding to rDer p 5. Five negative control sera from allergic patients with no IgE reactivity to natural Der p 1 and Der p 2 (measured by multiplex array technology) were tested. The remaining 62 sera were from patients sensitized to either Der p 1 or Der p 2 or both. In data not shown, twenty two of the 62 sera (35.5%) had IgE antibody binding to rDer p 5, in agreement with the range of reported prevalences of IgE antibody to this allergen (7,8,32,33), indicating that this construct is a good model of the natural allergen.

Crystal Structure- The structure of Der p 5 contains three helices connected by short loops. In the crystal structure determined here, the helices are splayed to interact with another Der p 5 molecule to form dimers. Figure 1a shows the six Der p 5 molecules in the asymmetric unit, arranged as a trimer of imperfectly matched dimers. The chains in the central dimer are designated A and B, while the peripheral dimers contain chains C paired with D and E paired with F. The N-terminus in the crystal form is exposed to the solvent channels suggesting these trimers of dimers are still possible in the full-length construct (Figure 1a). The A-B dimer is the best ordered in the structure (average B-factor 67.1) based on overall B factor analysis followed by C-D ($\langle B \rangle = 86.2$) and E-F ($\langle B \rangle = 101.4$). The two chains that make up the A-B dimer align very well, with an RMSD $< 0.5 \text{ \AA}$ but the same is not true of the C-D and E-F dimers. This indicates that the C-D and E-F dimers are not as symmetric as the A-B dimer. The C-D and E-F dimers are very similar as can be seen in Figure 1b ($C\alpha$ RMSD = 0.56 \AA over 191 atoms). Figure 1c shows the alignment of A-B with C-D, which do not align as well ($C\alpha$ RMSD = 3.2 \AA over 201 atoms). The N-terminal helix is significantly more bent in A-B, while all the helices in C-D and E-F appear straighter. The kink in the N terminal helix occurs at Gly45, which probably provides flexibility and confers upon Der p 5 a significant degree of conformational plasticity.

A particularly interesting feature of the Der p 5 dimer is the formation of a large hydrophobic pocket, Figure 2. The volume of the pocket ranges from 2960 to 3109 \AA^3 in the three dimers, evaluated by the program CastP (34). The values given should be considered approximate because it is unclear exactly where the pocket begins and ends. The pocket runs almost half the length of the dimers with openings to solvent at both ends of the cavity. The pockets contain ordered density, which was fit with water, phosphate, or MPD molecules, since all were present during crystallization. The greatest amount of ligand density was observed in the A-B dimer, and poorer density and/or fewer molecules were found in the C-D or E-F dimers. This result suggests that Der p 5 has the potential to bind hydrophobic ligands, which is a common feature of many allergens (35).

Relation to Blo t 5 Structures- Figure 3 compares the folding topology of the Der p 5 monomer of chain A with the Blo t 5 structures 2JMH and 2JRK (19,20). Viewed along an axis parallel to the main helical axes, the helices of 2JMH are arranged in a counterclockwise orientation, while the helices of 2JRK are arranged in a clockwise orientation. The two topologies thus approximate mirror images of each other. As a result of the 41% sequence identity between Der p 5 and Blo t 5, it was anticipated that the Der p 5 structure might shed light on this unexpected inconsistency between the two previously determined Blo t 5 structures. The fold topology of the Der p 5 monomer is counterclockwise like the 2JMH structure supporting this as the correct fold for group 5 proteins.

Analysis of Interfaces in the Crystal- A detailed analysis of the important residues for the various interfaces was provided using the program PISA (Protein Interfaces Surfaces and Assemblies) (36). The A-B dimer interface contains 11 hydrogen bonds and 6 salt bridges. With only one exception, all of these interactions are side-chain to side-chain as might be expected for interactions between helices. Similarly, the C-D and E-F dimer interfaces contain 14 and 6 hydrogen bonds and 6 and 2 salt bridges, respectively. In all three dimers the important residues for hydrophobic

interactions include M35 to F50, L34 to I115, and V88 to G84.

The inter-dimer interfaces also contain a number of hydrophobic contacts. Similar residues can be found at each interface, but in slightly different orientations, as can be seen in Figure 4. For example, common hydrophobic residues at each interface include L47, F50, Y51, I100, F101, and Y104 from different monomers as denoted with a subscript letter. Figures 4a and 4b compare the two dimer interfaces within the unit cell. There was very little electron density for several residues at the AB-EF interface so in figure 4b, these residues were modeled based on the best available rotamer to give perspective in the figure. Figure 4c shows that at the crystallographic interface between dimers C-D and E-F, similar hydrophobic residues can be found again.

The various interfaces were examined to evaluate the buried surface area and shape complementarity (37). Table 2 lists the intra-dimer interfaces, the inter-dimer interfaces, and the crystallographic interfaces for which there is significant contact within 4 Å. The average surface area reported is the average from the two partners. In general, the largest values of buried surface area exist between the intra-chain dimer surfaces which buries between 507-775 Å² with shape complementarity (SC) scores between 0.55 and 0.64. For comparison, antibody-antigen interactions typically involve 600-900 Å² and have shape complementarity (SC) scores of 0.6 (37). The inter-dimer interfaces that are non-crystallographic bury between 149 and 247 Å² per molecule, which is between a half and a third of that found for the intra-dimer interactions. Similarly, the crystallographic interface that would continue the hexameric pattern to the left or right in Figure 1 buries 199 Å². For each of these inter-dimer interactions the buried surface area is low but the shape complementarity is relatively high. Finally, there are AB-AB dimer contacts in the direction perpendicular to the page, which buries only 107 Å².

Characterization with SAXS- Small angle x-ray scattering was employed to determine the solution stoichiometry of Der p 5, using I_0 analysis. Table 3 shows the calculated molecular mass based on the average particle size in solution. The data suggests that a large fraction of Der p 5 is

monomeric at low concentrations. However, the average particle size of Der p 5 increases with concentration indicating a tendency to form oligomers. Consistent with this observation multiangle light scattering confirms that Der p 5 is predominantly monomeric in solution but exhibits a concentration dependent increase in apparent molecular weight from 14 to 19 kDa, where the actual MW is 12.0 kDa for the construct used here (data not shown).

SAXS data also contains information about molecular shapes, and given the crystal structure with a trimer of dimers, we assessed the relative populations of different multimeric structures that might be in solution. Figure 5a shows diagrams of the structures that were considered for evaluation: [1] a monomer with the structure of Der p 5 chain A, [2] a monomer like Blo t 5 (2JMH), [3] a Der p 5 dimer using chains A and B, [4] a dimer like Der p 21, [5] a tetramer using chains A, B, C, and D, [6] a hexamer of chains A, B, C, D, E, & F, [7] a dodecamer using two symmetry related hexamers, and [8] an 18mer using three symmetry related hexamers. Model [4] was based on *ab initio* modeling of SAXS data for Der p 21(21), which resembles a dimer between chains B and D. The experimental scattering curve was analyzed as a weighted contribution of the theoretical scattering from the 8 structure possibilities listed above using the program OLIGOMER (31). Figure 5b shows the fit to the data obtained at a concentration of 2.5mg/ml and Table 3 lists the results in conjunction with the average particle size. The analysis indicates that the primary solution structure is [2] a monomer like Blo t 5, which represents 54-74% of the species present depending on the concentration. At low concentrations, dimers shaped like the low resolution SAXS structure of Der p 21 constitute 4% of the population. Additionally there are hexamers and dodecamers that increase in relative population as the concentration of Der p 5 increases. At each concentration a weighted average of molecular mass based on the relative populations very closely matches the predicted particle size based on I_0 analysis (Table 3). As a control, we also attempted to simultaneously fit other structure possibilities like trimers and pentamers but these shapes were rejected by the OLIGOMER analysis (data not shown).

DISCUSSION

This paper presents the first crystal structure of a group 5 mite allergen, Der p 5 from *Dermatophagoides pteronyssinus*. A short construct was designed based on the available NMR Blo t 5 structures to decrease the number of disordered residues. The prevalence of IgE antibody binding to the shorter Der p 5 construct used here is the same as reported for the natural allergen, indicating that this construct is physiologically relevant. A previous study using peptides to map patient IgE epitopes on Blo t 5, found very few patients with high IgE reactivity to the N terminal peptides (19). This suggests that IgE antibodies are not directed against the flexible N-terminal residues of Der p 5, which are absent in the shorter construct.

The folding topology of the helices in Der p 5 is similar to that reported for the Blo t 5 solution structure (2JMH) and differs from the reported structure (2JRK). The most likely interpretation of the discrepancy is that the predicted NOE differences were sufficiently small so that an incorrect structure was obtained in one of the studies. Indeed, when we examined the reported distance restraints for 2JMH, approximately 90% were satisfied in the 2JRK structure (data not shown). Generally there is enough information in the NOE data to differentiate between these possibilities, but a 3 helical bundle represents a challenging situation where errors have been known to occur (38,39). Given the degree of sequence identity between Blo t 5 and Der p 5, we suggest that the structure 2JMH is most likely to be correct.

The results of the SAXS data show a large population of Der p 5 to be monomeric in solution although Der p 5 appears to show concentration dependent oligomerization (Table 3). The asymmetric unit of the Der p 5 crystal is a hexamer, which consists of an imperfect trimer of dimers, while Blo t 5 is reported to be a monomer (20). The discovery of a multimeric form of Der p 5 is not unprecedented in the literature. In a previous crystallization report, the Matthew's coefficient predicted that the unit cell could accommodate 12 molecules per asymmetric unit (22). The crystals were grown at low pH and subsequent studies of Der p 5 reported a strong

tendency to polymerize in acidic conditions (23). At neutral pH (7.4) and low concentrations, the protein was largely monomeric, but some dimers could be detected in cross linking studies. Small angle X-ray studies of Der p 21 (34% identity to Der p 5, Figure 6) indicated that the Der p 21 allergen was dimeric (21). Studies of immunostained mites noted that Der p 5 appeared on fibrous structures in the food ball (10). In combination with the present results, these observations suggest that Der p 5 may be an integral structural component of these fibers given the apparent proclivity to polymerize. It is also conceivable that given the similarities between Der p 5 and Der p 21, both could be involved in forming polymers.

An interesting question is whether or not other group 5 and group 21 allergens could polymerize similarly to what the crystal structure and past biochemical analysis of Der p 5 supports, bearing in mind biophysical data indicates Blo t 5 to be monomeric (20). Figure 6 presents a multiple sequence alignment of Der p 5, Blo t 5, Der p 21, and Blo t 21. Residues that are strongly conserved in the intra-dimer and inter-dimer interfaces are shown in color. Residue G46, which appears important for the flexibility of the N terminal helix, is conserved in Blo t 5 and Der p 5, but not in the group 21 allergens. Many of the other residues that are important for intra- and inter-dimer interactions are highly conserved. The most compelling distinction that might provide a basis for the preference of Blo t 5 to not polymerize appears to be related to the sequence 84-88, which is GVRGV in Der p 5 and is GAQGA in Blo t 5. In the dimeric structure of Der p 5 this helical sequence interacts in an antiparallel manner with itself. Residue V88 from one chain fits into a notch created by G84 of the other chain, with V85 contributing hydrophobic interactions to create a "valine zipper" (analogous to a leucine zipper) at the intra-dimer interface. In Blo t 5 these residues are alanines, which may not contribute enough hydrophobic surface to stabilize a dimer. However the group 21 allergens have a bulky side-chain at the comparative position 88, and a smaller side-chain at 85 (A or S), so one could imagine the intra-dimer interactions forming. A monomer of Der p 5 like that found in the crystal is not found in the SAXS analysis possibly because the first helix in the molecules

are “splayed” in the crystal dimer and not straight like the more compact monomeric Blo t 5 structure.

The cavity observed in the Der p 5 dimer is particularly interesting, considering the existence of many allergens with hydrophobic cavities that bind lipid-like ligands. For example the cat allergen Fel d 1 binds steroid-like molecules (40), the horse allergen Equ c 1 and the mouse allergen Mus m 1 are lipocalins (41,42), and Der f 2 was demonstrated to bind lipopolysaccharide (LPS) (43). Interestingly, the crystal structures of both Der p 2 and Bet v 1 contained apparent ligands in a hydrophobic environment with difficult to interpret electron density (44,45). The connection of hydrophobic ligand binding to allergy is thought to be related to hydrophobic compounds from bacteria that are commonly recognized by the innate immune system (18). It has been suggested that allergens carrying hydrophobic compounds shift the

immune response from tolerance to Th2 type immune responses that are associated with allergic inflammation (46). The function of several dust mite allergens support this contention. For example Der p 2 functionally substituted for murine MD-2, an innate immune protein known to bind LPS from gram negative bacteria (18). Similarly, the structure of Der p 7 resembles LPS binding protein (LBP) and Der p 7 was shown to bind a lipopeptide from gram positive bacteria (17). The structure of Der p 5 presented here suggests that a Der p 5 dimer may also have a propensity to bind hydrophobic compounds. Future studies are planned to investigate ligand binding in an effort to better understand the natural function of this important allergen and to determine whether this function is related to its allergenicity. We hypothesize that hydrophobic ligands or the natural ligand could induce a structural change to encourage dimer formation as seen in the crystal.

REFERENCES

1. Sporik, R., Chapman, M. D., and Platts-Mills, T. A. (1992) *Clin Exp Allergy* **22**(10), 897-906
2. Chapman, M. D., Pomes, A., Breiteneder, H., and Ferreira, F. (2007) *Journal of Allergy and Clinical Immunology* **119**(2), 414-420
3. Thomas, W. R., and Hales, B. J. (2007) *Immunol Res* **37**(3), 187-199
4. Arruda, L. K., Rizzo, M. C., Chapman, M. D., Fernandez-Caldas, E., Baggio, D., Platts-Mills, T. A., and Naspitz, C. K. (1991) *Clin Exp Allergy* **21**(4), 433-439
5. Caraballo, L., Puerta, L., Fernandez-Caldas, E., Lockey, R. F., and Martinez, B. (1998) *J Investig Allergol Clin Immunol* **8**(5), 281-284
6. Arruda, L. K., Vailes, L. D., Platts-Mills, T. A., Fernandez-Caldas, E., Montealegre, F., Lin, K. L., Chua, K. Y., Rizzo, M. C., Naspitz, C. K., and Chapman, M. D. (1997) *Am J Respir Crit Care Med* **155**(1), 343-350
7. Simpson, A., Green, R., Custovic, A., Woodcock, A., Arruda, L. K., and Chapman, M. D. (2003) *Allergy* **58**(1), 53-56
8. Chew, F. T., Yi, F. C., Chua, K. Y., Fernandez-Caldas, E., Arruda, L. K., Chapman, M. D., and Lee, B. W. (1999) *Clin Exp Allergy* **29**(7), 982-988
9. Kuo, I. C., Cheong, N., Trakultivakorn, M., Lee, B. W., and Chua, K. Y. (2003) *J Allergy Clin Immunol* **111**(3), 603-609
10. Weghofer, M., Grote, M., Dall'Antonia, Y., Fernandez-Caldas, E., Krauth, M. T., van Hage, M., Horak, F., Thomas, W. R., Valent, P., Keller, W., Valenta, R., and Vrtala, S. (2008) *Int Arch Allergy Immunol* **147**(2), 101-109
11. Chapman, M. D., Wunschmann, S., and Pomes, A. (2007) *Current Allergy and Asthma Reports* **7**(5), 363-367
12. King, C., Brennan, S., Thompson, P. J., and Stewart, G. A. (1998) *J Immunol* **161**(7), 3645-3651
13. Tomee, J. F., van Weissenbruch, R., de Monchy, J. G., and Kauffman, H. F. (1998) *J Allergy Clin Immunol* **102**(1), 75-85
14. Hewitt, C. R., Brown, A. P., Hart, B. J., and Pritchard, D. I. (1995) *J Exp Med* **182**(5), 1537-1544
15. Schulz, O., Sewell, H. F., and Shakib, F. (1998) *J Exp Med* **187**(2), 271-275

16. Kauffman, H. F., Tamm, M., Timmerman, J. A., and Borger, P. (2006) *Clin Mol Allergy* **4**, 5
17. Mueller, G. A., Edwards, L. L., Aloor, J. J., Fessler, M. B., Glesner, J., Pomes, A., Chapman, M. D., London, R. E., and Pedersen, L. C. (2010) *Journal of Allergy and Clinical Immunology* **125**(4), 909-917
18. Trompette, A., Divanovic, S., Visintin, A., Blanchard, C., Hegde, R. S., Madan, R., Thorne, P. S., Wills-Karp, M., Gioannini, T. L., Weiss, J. P., and Karp, C. L. (2009) *Nature* **457**(7229), 585-588
19. Chan, S. L., Ong, T. C., Gao, Y. F., Tiong, Y. S., Wang de, Y., Chew, F. T., and Mok, Y. K. (2008) *J Immunol* **181**(4), 2586-2596
20. Naik, M. T., Chang, C. F., Kuo, I. C., Kung, C. C., Yi, F. C., Chua, K. Y., and Huang, T. H. (2008) *Structure* **16**(1), 125-136
21. Weghofer, M., Dall'Antonia, Y., Grote, M., Stocklinger, A., Kneidinger, M., Balic, N., Krauth, M. T., Fernandez-Caldas, E., Thomas, W. R., van Hage, M., Vieths, S., Spitzauer, S., Horak, F., Svergun, D. I., Konarev, P. V., Valent, P., Thalhamer, J., Keller, W., Valenta, R., and Vrtala, S. (2008) *Allergy* **63**(6), 758-767
22. Liaw, S. H., Chen, H. Z., Kuo, I. C., and Chua, K. Y. (1998) *J Struct Biol* **123**(3), 265-268
23. Liaw, S. H., Chen, H. Z., Liu, G. G., and Chua, K. Y. (2001) *Biochem Biophys Res Commun* **285**(2), 308-312
24. Otwinowski, Z., and Minor, W. (1997) *Macromolecular Crystallography, Pt A* **276**, 307-326
25. Kabsch, W. (2010) *Acta Crystallographica Section D-Biological Crystallography* **66**, 133-144
26. Zwart, P. H., Afonine, P. V., Grosse-Kunstleve, R. W., Hung, L. W., Ioerger, T. R., McCoy, A. J., McKee, E., Moriarty, N. W., Read, R. J., Sacchettini, J. C., Sauter, N. K., Storoni, L. C., Terwilliger, T. C., and Adams, P. D. (2008) *Methods Mol Biol* **426**, 419-435
27. Emsley, P., and Cowtan, K. (2004) *Acta Crystallographica Section D-Biological Crystallography* **60**, 2126-2132
28. Brunger, A. T., Adams, P. D., Clore, G. M., DeLano, W. L., Gros, P., Grosse-Kunstleve, R. W., Jiang, J. S., Kuszewski, J., Nilges, M., Pannu, N. S., Read, R. J., Rice, L. M., Simonson, T., and Warren, G. L. (1998) *Acta Crystallographica Section D-Biological Crystallography* **54**, 905-921
29. Konarev, P. V., Volkov, V. V., Sokolova, A. V., Koch, M. H. J., and Svergun, D. I. (2003) *J. Appl. Cryst.* **36**, 1277-1282
30. Svergun, D. I. (1992) *J. Appl. Cryst.* **25**, 495-503
31. Konarev, P. V., Volkov, V. V., Sokolova, A. V., Koch, M. H. J., and Svergun, D. I. (2003) *Journal of Applied Crystallography* **36**, 1277-1282
32. Caraballo, L., Mercado, D., Jimenez, S., Moreno, L., Puerta, L., and Chua, K. Y. (1998) *Int Arch Allergy Immunol* **117**(1), 38-45
33. Lin, K. L., Hsieh, K. H., Thomas, W. R., Chiang, B. L., and Chua, K. Y. (1994) *Journal of Allergy and Clinical Immunology* **94**(6), 989-996
34. Dundas, J., Ouyang, Z., Tseng, J., Binkowski, A., Turpaz, Y., and Liang, J. (2006) *Nucleic Acids Research* **34**, W116-W118
35. Radauer, C., Bublin, M., Wagner, S., Mari, A., and Breiteneder, H. (2008) *J Allergy Clin Immunol* **121**(4), 847-852 e847
36. Xu, Q., Canutescu, A. A., Wang, G., Shapovalov, M., Obradovic, Z., and Dunbrack, R. L., Jr. (2008) *J Mol Biol* **381**(2), 487-507
37. Lawrence, M. C., and Colman, P. M. (1993) *J Mol Biol* **234**(4), 946-950
38. DeRose, E. F., Kirby, T. W., Mueller, G. A., Chikova, A. K., Schaaper, R. M., and London, R. E. (2004) *Structure* **12**(12), 2221-2231
39. Mueller, G. A., Kirby, T. W., DeRose, E. F., Li, D. W., Schaaper, R. M., and London, R. E. (2005) *Journal of Bacteriology* **187**(20), 7081-7089
40. Kaiser, L., Gronlund, H., Sandalova, T., Ljunggren, H. G., van Hage-Hamsten, M., Achour, A., and Schneider, G. (2003) *J Biol Chem* **278**(39), 37730-37735

41. Lascombe, M. B., Gregoire, C., Poncet, P., Tavares, G. A., Rosinski-Chupin, I., Rabillon, J., Goubran-Botros, H., Mazie, J. C., David, B., and Alzari, P. M. (2000) *J Biol Chem* **275**(28), 21572-21577
42. Bocskei, Z., Groom, C. R., Flower, D. R., Wright, C. E., Phillips, S. E., Cavaggioni, A., Findlay, J. B., and North, A. C. (1992) *Nature* **360**(6400), 186-188
43. Ichikawa, S., Takai, T., Yashiki, T., Takahashi, S., Okumura, K., Ogawa, H., Kohda, D., and Hatanaka, H. (2009) *Genes Cells* **14**(9), 1055-1065
44. Derewenda, U., Li, J., Derewenda, Z., Dauter, Z., Mueller, G. A., Rule, G. S., and Benjamin, D. C. (2002) *J Mol Biol* **318**(1), 189-197
45. Gajhede, M., Osmark, P., Poulsen, F. M., Ipsen, H., Larsen, J. N., Joost van Neerven, R. J., Schou, C., Lowenstein, H., and Spangfort, M. D. (1996) *Nat Struct Biol* **3**(12), 1040-1045
46. Thomas, W. R., Hales, B. J., and Smith, W. A. (2005) *Current Allergy and Asthma Reports* **5**(5), 388-393

FOOTNOTES

The authors wish to thank Doan-Thu Nguyen, Cynthia Holley, and Andrea Moon for helpful contributions, and Dr. Lin Yang at the National Synchrotron Light Source at Brookhaven National Laboratory, for assistance with data collection. We are grateful to Dr. Wayne Thomas (Western Australian Research Institute for Child Health, Perth, Western Australia) for providing the pGEX Der p 5 construct.

The project described was supported in part by the Intramural Research Program of the National Institutes of Health (NIH), National Institute of Environmental Health Sciences, and by Award Number R01AI077653 from the National Institute Of Allergy And Infectious Diseases (A.P. and M.D.C.). The content is solely the responsibility of the authors and does not necessarily represent the official views of the National Institute of Allergy and Infectious Diseases or the National Institutes of Health. Use of the X9 beamline at National Synchrotron Light Source at Brookhaven National Laboratory is supported by the United States Department of Energy, Office of Science, Office of Basic Energy Sciences, under Contract DE-AC02-98CH10886. J.M.K.'s contribution was funded in whole with federal funds from the National Institutes of Health, National Institute of Environmental Health Sciences, under Delivery Order HHSN273200700046U to SRA International, Inc.

All NIEHS authors declare they have no potential competing financial interest. Martin. D. Chapman is an owner of Indoor Biotechnologies, Inc, Charlottesville, VA, and Anna Pomés in an employee of Indoor Biotechnologies Inc.

The abbreviations used are: SAXS, small angle x-ray scattering; GST, glutathione S-transferase; TEV, tobacco etch virus; SC, shape complimentarity; lipopolysaccharide (LPS); NOE, nuclear Overhauser effect; MPD, methylpentanediol.

FIGURE LEGENDS

Fig. 1. Assymmetric unit of the Der p 5 crystal structures- a. Hexamer of Der p 5- There are six molecules of Der p 5 in the asymmetric unit of the crystal forming a trimer of dimers. The N terminus is designated, as well as the chain name of the molecules. b. Alignment of the C-D and E-F dimers. c. Alignment of the A-B and C-D dimers. The PDB code for the Der p 5 structure is 3MQ1.

Fig. 2. Cavity in the Der p 5 dimer- a. The cavity in the A-B dimer is rendered with a solid surface and the helices in the asymmetric unit are rendered as semi-transparent ribbons. b. Zoomed region of panel a.

Ordered density in the cavity was assumed to be either water or MPD however the electron density is poorly determined so it is rendered with a solid surface just to give an impression of the size of the cavity.

Fig. 3. Comparisons of Der p 5 with published Blo t 5 structures- The monomeric form of Der p 5 from chain A is displayed in panel a. Panel b shows the first structure from 2JMH and panel c is the first structure from 2JRK. Helix 1 is red, helix 2 is blue, and helix 3 is green. Circles at the bottom indicate the “handedness” of the structures, looking “down” the helical axis.

Fig. 4. Important residues for various inter-dimer interfaces. Panel a shows the interface between A-B and C-D, panel b shows the interface between A-B and E-F, and panel c shows a crystallographic interface between C-D and E-F. Note that similar residues appear at each interface but in different conformations. Residues rendered with a thin line lack electron density and are modeled based on best allowed rotamer. F50_F has two conformations in the crystal structure.

Fig. 5. SAXS analysis- Panel a shows the eight tested structures for fit to the SAXS data as described in the text. Panel b shows the theoretical fit of the SAXS data (red line) to the acquired scattering data (black squares with error bars) for the 2.5 mg/ml sample of Der p 5, inset with the linear region of the Guinier fit. Panel c shows the P(r) plot for the same sample.

Fig. 6. Sequence Comparisons- ClustalW alignments of Der p 21, Blo t 21, Blo t 5, and Der p 5 are shown. Color red are residues important for the Der p 5 intra-dimer interface, blue are residues important for inter-dimer interfaces, and green are residues involved in both types of interfaces. Asterisks indicate identity, colons indicate strong similarity, and periods indicate weaker similarity among the four proteins.

Table 1:

Crystallographic data statistics			
data set	Native	Se-met (peak)	Se-met (edge)
Wavelength (Å)	1.5418	0.97243	0.97943
unit cell (a,b,c) (Å)	46.78, 96.57, 167.89	46.78, 96.70, 168.14	46.77, 96.64, 168.13
Space Group	P2 ₁ 2 ₁ 2 ₁	P2 ₁ 2 ₁ 2 ₁	P2 ₁ 2 ₁ 2 ₁
Resolution (Å)	50-2.8	50-2.7	50-2.7
# of observations	124140	22515	22461
unique reflections	19292	254289	271926
R _{sym} (%) ^{1,2}	6.9 (51.8)	14.7 (50.4)	13.7 (55.0)
I/σI	15.7 (2.5)	15.1 (2.2)	12.1 (2.1)
Mosaicity range	1.3 -1.6	0.4-1.9	0.4-1.3
completeness(%)	98.8 (98.5)	99.0 (90.6)	98.7 (89.2)
<u>Refinement statistics</u>			
R _{cryst} ³ , R _{free} ⁴ (%)	22.6,27.9		
# of waters	45		
Overall Wilson B value (Å ²)	62.5		
Average B for:			
molecules A,B	67.1		
molecules C,D	86.2		
molecules E,F	101.4		
water	69.0		
<u>r.m.s.d from ideal values</u>			
bond length (Å)	0.001		
bond angle (°)	0.307		
dihedral angle (°)	8.78		
<u>Ramachandran Statistics⁵</u>			
favored (98%) regions (%)	98.0		
allowed (>99.8%) regions (%)	99.8		
1) Se-met data were scaled by merging Friedel pairs but I+ and I- were written out separately.			
1) R _{sym} = $\sum (I_i - \langle I \rangle) / \sum (I_i)$ where I _i is the intensity of the ith observation and $\langle I \rangle$ is the mean intensity of the reflection.			
2) last resolution shell is in ().			
3) R _{cryst} = $\sum F_o - F_c / \sum F_o $ calculated from working data set.			
4) R _{free} was calculated from 5% of data randomly chosen not to be included in refinement.			
5) Ramachandran results were determined by MolProbity.			

Table 2: Interface Summary

Interface	Chains	<SurfaceArea> (Å ²)	Shape Complimentarity
Intra-chain	AB	755	0.63
	CD	715	0.64
	EF	509	0.55
Inter-chain	AB-CD	246	0.69
	AB-EF	150	0.64
Crystallographic	CD-EF	199	0.56
	AB-AB	107	0.66

Table 3: SAXS analysis

Der p 5 Concentration (mg/ml)	2.5	5	10
<i>I</i>₀ Analysis			
MM (kDa)	43.5	59.9	82.6
OLIGOMER Analysis of Relative Populations*			
1. Der p 5- like monomer	0.0%	0.0%	0.0%
2. Blo t 5-like monomer	74.0%	65.0%	54.1%
3. Der p 5 – AB- dimer	0.0%	0.0%	0.0%
4. Der p 21-like dimer	4.1%	0.0%	0.0%
5. Der p 5 tetramer (AB and CD)	0.0%	0.0%	0.0%
6. Der p 5 hexamer	20.3%	30.7%	32.6%
7. Der p 5 dodecamer	1.5%	4.3%	13.3%
8. Der p 5 “18mer”	0.0%	0.0%	0.0%
MM (kDa) Weighted average of populations	44.1	63.9	85.6
χ ² Oligomer Fit	1.5	3.3	11.1

* See text for more description and Figure 5a for visual depictions of models.

Figure 1

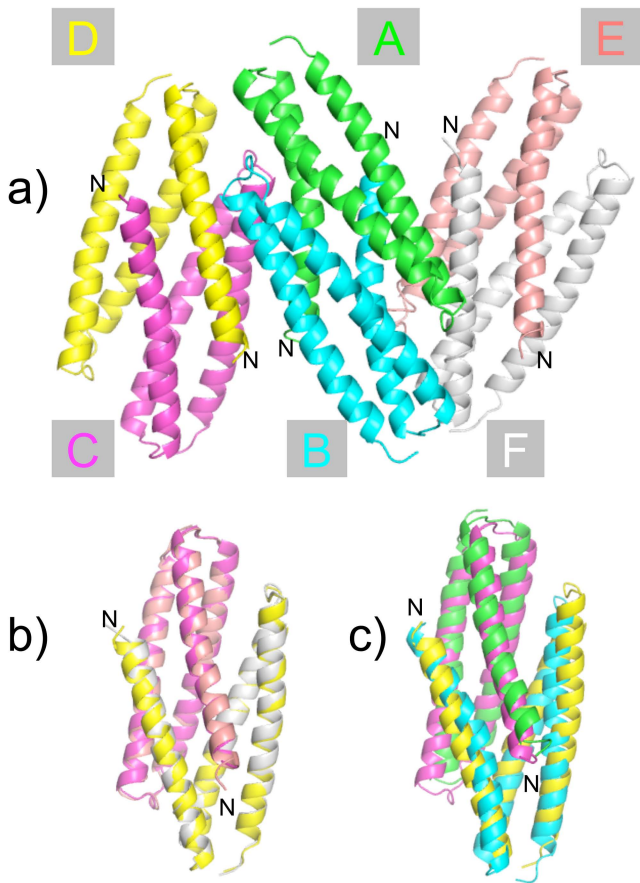


Figure 2

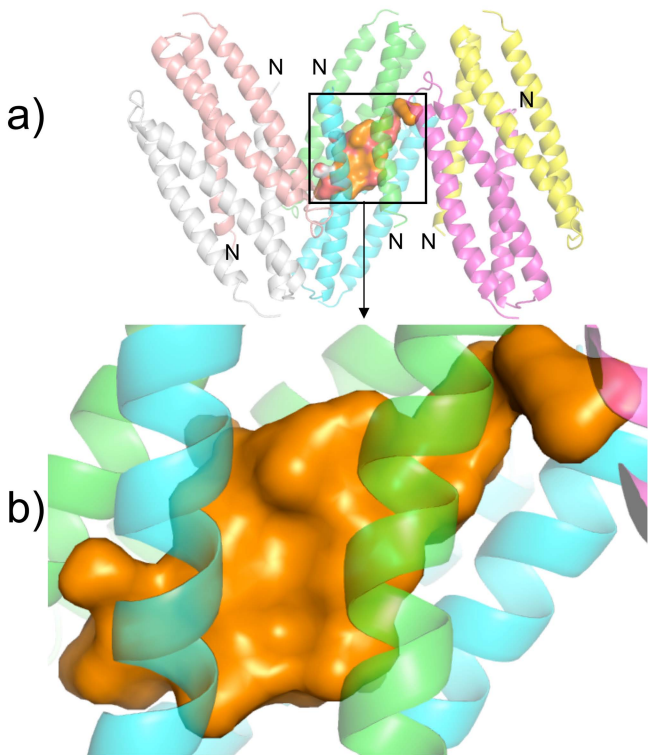
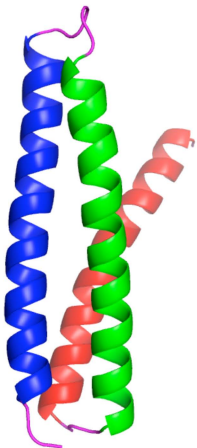
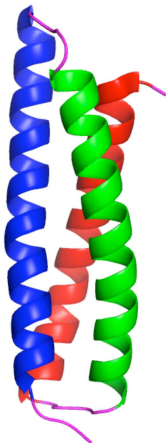


Figure 3

a) Der p 5



b) Blo t 5
2JMH



c) Blo t 5
2JRK

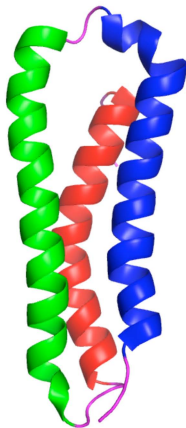


Figure 4

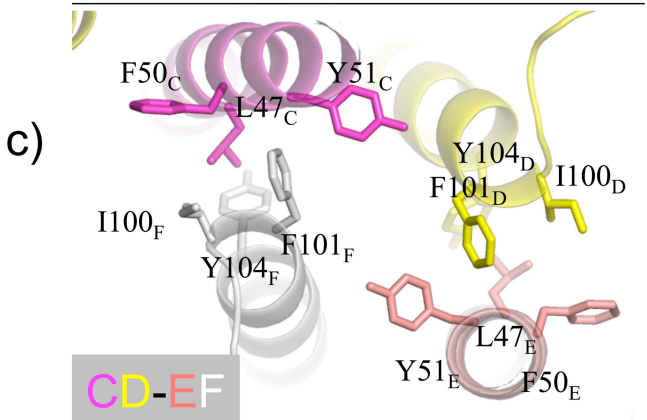
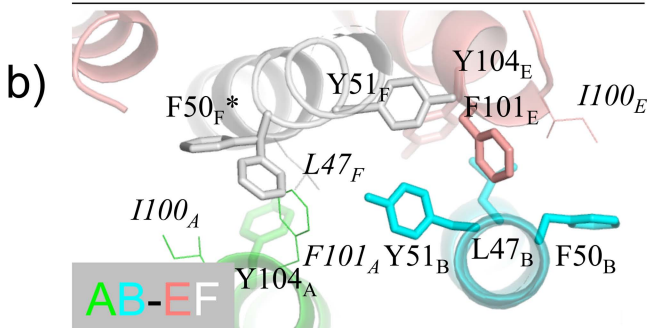
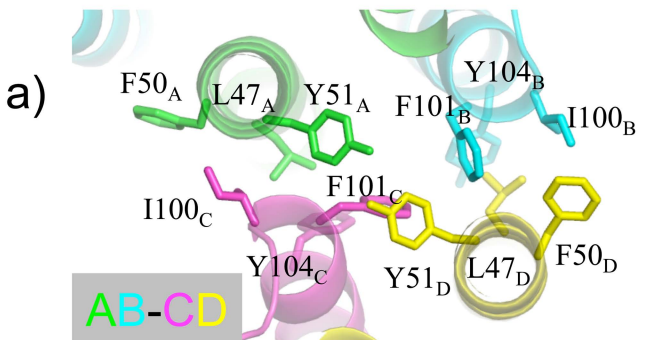


Figure 5

